

Compressed Skinning for Facial Blendshapes

Ladislav Kavan
lkavan@meta.com
Meta
Zürich, Switzerland

John Doublestein
jdoublestein@meta.com
Meta
Redmond, USA

Martin Prazak
map@meta.com
Meta
Zürich, Switzerland

Matthew Cioffi
mail@mattcioffi.com
Meta
Londonderry, USA

Doug Roble
droble@acm.org
Meta
Sausalito, USA

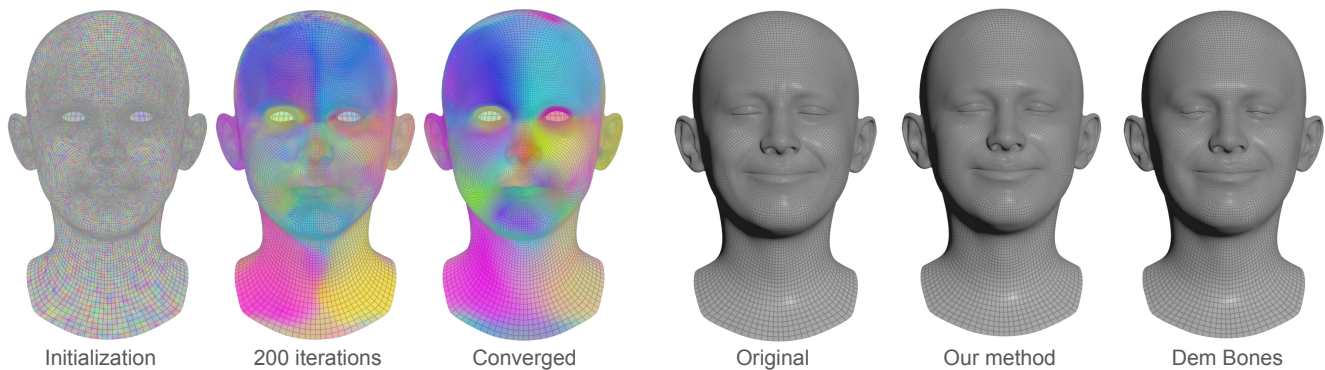


Figure 1: Starting from a random initialization of skinning weights, our method converges to a linear blend skinning approximation of input blendshapes. The accuracy and visual quality of our results is comparable to the state-of-the-art (Dem Bones), but introduces significantly smaller run-time overheads. In the figure, each color visualizes the influence of one bone, with 40 bones total.

ABSTRACT

We present a new method to bake classical facial animation blendshapes into a fast linear blend skinning representation. Previous work explored skinning decomposition methods that approximate general animated meshes using a dense set of bone transformations; these optimizers typically alternate between optimizing for the bone transformations and the skinning weights. We depart from this alternating scheme and propose a new approach based on proximal algorithms, which effectively means adding a projection step to the popular Adam optimizer. This approach is very flexible and allows us to quickly experiment with various additional constraints and/or loss functions. Specifically, we depart from the classical skinning paradigms and restrict the transformation coefficients to contain only about 10% non-zeros, while achieving similar accuracy and visual quality as the state-of-the-art. The sparse storage enables our method to deliver significant savings in terms of both memory and run-time speed. We include a compact implementation of our

new skinning decomposition method in PyTorch, which is easy to experiment with and modify to related problems.

CCS CONCEPTS

• **Computing methodologies** → **Animation.**

KEYWORDS

facial animation, blendshapes, skinning decomposition

ACM Reference Format:

Ladislav Kavan, John Doublestein, Martin Prazak, Matthew Cioffi, and Doug Roble. 2024. Compressed Skinning for Facial Blendshapes. In *Special Interest Group on Computer Graphics and Interactive Techniques Conference Conference Papers '24 (SIGGRAPH Conference Papers '24)*, July 27-August 1, 2024, Denver, CO, USA. ACM, New York, NY, USA, 9 pages. <https://doi.org/10.1145/3641519.3657477>

1 INTRODUCTION

Many people can access interactive graphics only through inexpensive handheld devices, which is problematic for delivering appealing animated 3D characters. While cloud compute is one potential solution, scaling graphics workloads to billions of users would require a prohibitive amount of compute resources. Therefore, on-device execution is the most viable path to deliver interactive 3D experiences to a large user base. Artists working with facial animation and

Permission to make digital or hard copies of part or all of this work for personal or classroom use is granted without fee provided that copies are not made or distributed for profit or commercial advantage and that copies bear this notice and the full citation on the first page. Copyrights for third-party components of this work must be honored. For all other uses, contact the owner/author(s).

SIGGRAPH Conference Papers '24, July 27-August 1, 2024, Denver, CO, USA

© 2024 Copyright held by the owner/author(s).

ACM ISBN 979-8-4007-0525-0/24/07.

<https://doi.org/10.1145/3641519.3657477>

rigging usually seek maximum creative control and flexibility. This often leads to the use of a large number of blendshapes. High-end film rigs use over 1000 blendshapes, and even less detailed stylized characters still require about 200-300 blendshapes, especially due to corrective shapes needed to overcome the limitations of linear blending.

Many data compression algorithms have been studied in the past, but real-time animation requires a decompression method that is fast and integrates well with a GPU that performs the final rendering. Linear blend skinning decomposition methods [James and Twigg 2005] have been proposed to solve this problem for general animated meshes and they also work well for facial blendshapes. Linear blend skinning decomposition departs from the traditional hierarchical skeleton structures and instead approximates an input data matrix $A \in \mathbb{R}^{3S \times N}$ as a product of two factors: $A \approx BC$, where $B \in \mathbb{R}^{3S \times 4P}$, $C \in \mathbb{R}^{4P \times N}$. The input matrix A contains the x , y , z coordinates of the S input shapes with N vertices; the P is the number of proxy-bones. The matrices B and C have special structure: B is typically dense and stacks the skinning transformations; C is typically sparse and combines the skinning weights with the rest pose. The problem of “skinning decomposition” can be defined as finding the factors B and C for a given A . The state-of-the-art method for solving this problem is implemented in the open source “Dem Bones” library [Electronic Arts [n. d.]; Le and Deng 2012] which has been integrated in Maya, Houdini and many other tools. Linear blend skinning is a widely recognized standard in interactive graphics. By adhering to this standard, we can take advantage of highly optimized shader implementations, file formats, and tools that are already in place.

In Dem Bones, as well as in most publications on this problem, the user has to select a fixed number of proxy-bones. These proxy-bones do not have any anatomical meaning, but they correspond to individual skinning transformations; each transformation drives part of the mesh. With our rigs, we found that as few as 40 proxy-bones lead to acceptable quality with Dem Bones. However, even with a modest set of 300 blendshapes, this introduces significant run-time overheads, because for each of the shapes we need to store all of the proxy-bone transformations: $300 \times 40 = 12000$ (with each individual transformation represented either via a 3×4 matrix or a [quaternion, translation] pair). These transformations have to be read and blended at run-time for each character, every frame. We can do better if we revisit the problem of skinning decomposition from scratch. Previous work explored solvers based on alternating between optimization for the skinning weights and the transformations (cyclic coordinate descent). More and more efficient and general solvers were explored during the 2005 - 2015 decade and open sourced in 2019 in the Dem Bones library. The need to minimize the run-time compute requirements lead us to explore an entirely different optimization strategy, motivated by the success of first-order optimization methods used in deep learning. This is not trivial, because typical deep learning optimizers assume unconstrained optimization and typically handle bounds via sigmoid or softmax functions. This may be sufficient for non-negativity and affinity of the skinning weights, but the hard constraint of spatial sparsity is more difficult. Inspired by proximal algorithms, well studied in the convex setting [Parikh et al. 2014], we append a

constraint-projection step to the popular Adam optimizer [Kingma and Ba 2014]; this is a key ingredient of our proposed method.

We are solving exactly the same optimization objective (loss) as previous skinning decomposition methods, including Dem Bones. However, this objective is highly non-convex and thus different optimization methods converge to different solutions. Our approach consistently converges to solutions with lower errors than the Dem Bones solver. We can even lower the number of proxy-bones to 20 and still obtain similar accuracy as Dem Bones, but we needed more significant savings. Our key finding to report in this paper is that we can introduce sparsity constraints also on the transformations, i.e., zero-out about 90% of the coefficients of B and still match the accuracy of the Dem Bone results (this is in addition to the sparsity of C , i.e., both B and C are now sparse). This additional sparsification is straightforward to implement as part of the constraint-projection step. Even when accounting for the overhead of sparse data structures, this represents significant savings at runtime. To our knowledge, this additional “skinning transformation sparsification” has not been explored before and we propose to name it “compressed skinning” to distinguish it from previous skinning decomposition methods which compute dense B .

Our strategy of leveraging deep learning optimizers allows for a compact implementation in PyTorch [Paszke et al. 2019] with automatic backward differentiation and trivial deployment to CUDA. There are also additional benefits: previous skinning optimization methods start with a sophisticated initial guess computed with spectral or k-means clustering. With our approach, we simply use the Gaussian noise to initialize all of our variables (Figure 1) – more complicated initializations were not necessary and can introduce bias or even lead to worse results (e.g. in the case of symmetries preserved by the optimizer). Another advantage of our approach is its flexibility, e.g., changing the loss function is just a simple one-line code modification. We leveraged this flexibility and tried improving the accuracy of our fits by changing the error metric from the classical L^2 norm to an L^p norm with higher p . When we changed the norm to L^{12} and increased the number of influences to 32, the maximal error dropped by more than 50 times compared to Dem Bones, allowing us to recover even fine wrinkles in the original blendshapes, at the cost of more non-zeros weights in matrix C . However, our main focus is not improvements of quality but rather run-time efficiency.

Another contribution is a precise formulation of converting the “blend-weights” (i.e. the time-varying blendshape coefficients) to linear blend skinning transformations. This problem was not considered in previous skinning decomposition methods [James and Twigg 2005; Le and Deng 2012] which were more general and not focused on blendshape animation. This conversion is not hard but also it is not trivial because 1) skinning handles the rest pose differently than blendshapes and 2) linear blending of transformations is correct only when using a carefully chosen subset of spatial transformations (specifically, we use linearized rotations). Our first-order optimization approach requires longer pre-processing time than Dem Bones (on the order of minutes on a single GPU), but reduces the computation footprint on target devices.

Our main technical contributions are:

- New, first-order optimization method that solves skinning decomposition better than previous methods
- New skinning decomposition constraint: sparsity of transformations (“compressed skinning”)
- Explicit formulas to convert facial animation blend-weights into skinning transformations

However, our method is more complex than classical linear blend skinning and drifts away from established practices, in particular:

- Our method needs an extra sparse matrix-vector multiplication on the CPU to compute skinning transformations.
- The GPU skinning shaders need to support arbitrary transformation matrices (rig transformations are not sufficient).

2 BACKGROUND AND RELATED WORK

Traditional facial blendshape models are typically rooted in Facial Action Coding System [Ekman and Friesen 1978] or its variants [Lewis et al. 2014], though more recent research aims at addressing their limitations: complex controls and large number of blendshapes needed for high fidelity [Choi et al. 2022; Kim and Singh 2021]. If training data or facial rigs are available, it is possible to derive more efficient models using classical statistical methods [Meyer and Anderson 2007] or deep learning [Bailey et al. 2020; Chandran et al. 2022]. Our approach builds upon deep learning optimizers (Adam), but utilizes only the classical linear blend skinning model – no neural networks.

The problem of skinning decomposition was introduced by [James and Twigg 2005] and considered general animation sequences, not just facial animation, but also e.g. cloth animation or stylized full-body characters. Subsequent research led to better approximations of the unknown global optimum [Kavan et al. 2010], studied the benefits of adding bone rigidity constraints [Kavan et al. 2007; Le and Deng 2012] and further compression of the skinning weights via two-layer skinning [Le and Deng 2013]. All of the these methods find a cloud of unstructured proxy-bone transformations. An alternative approach aims to fit input animations with hierarchical skeletons [Bharaj et al. 2012; Hasler et al. 2010; Moutafidou et al. 2023; Schaefer and Yuksel 2007] which offers better editability and compatibility with tools such as Maya with well established support for hierarchical skeletons. Even though hierarchical skeletons are most commonly used for full-body animation, they can be also useful in facial animation, e.g. for the jaw and the eyes [Li et al. 2017]. However, high quality jaw opening can be also achieved without any skeleton using “intermediate” blendshapes [Lewis et al. 2014]. [Seo et al. 2011] studied blendshape compression via hierarchical semi-separable matrices, which finds permutations of the blendshape matrix and a tree structure eliminating blocks of zeros. This leads to a compact representation, but their method is closed-source and the decompression algorithm is much more complex than skinning. More recently, GPU-specific methods to speed up blendshape evaluation using compute shaders were proposed [Costigan et al. 2016].

Beyond computer graphics, methods such as Lasso [Tibshirani 1996], non-negative matrix factorization [Hoyer 2004; Lee and Seung 1999] and overcomplete dictionary learning [Aharon et al. 2006] discover sparse structures in input data. Compressed sensing [Donoho 2006] solves underdetermined linear systems by assuming

sparsity. The common theme in these methods are sparsity-inducing norms. The idea of combining the Adam optimizer with a proximal operator has been studied for the source separation problems in astronomical imaging [Melchior et al. 2019]. Each domain (structured data / images / meshes) has its own specifics. In the context of animated polygon meshes with constant connectivity, a scenario similar to ours, the L^1 norm has been utilized to transform an input mesh animation into a blendshape representation [Neumann et al. 2013]. However, our approach differs in that we take blendshapes as input and convert them into skinning. In other words, our method could potentially follow [Neumann et al. 2013] or any other method that generates blendshapes.

2.1 Blendshape Facial Models

In this section we briefly recap standard methods for facial blendshape modeling and establish notation for future sections. The classical blendshape model [Lewis et al. 2014] uses the following “delta” formulation centered at the rest-pose (neutral facial expression):

$$\hat{\mathbf{v}}_{0,i} + \sum_{k=1}^S c_k (\hat{\mathbf{v}}_{k,i} - \hat{\mathbf{v}}_{0,i}) \quad (1)$$

where $\hat{\mathbf{v}}_{0,i} \in \mathbb{R}^3$ is i -th rest-pose vertex, $\hat{\mathbf{v}}_{k,i} \in \mathbb{R}^3$ is i -th vertex in blendshape number k and c_k are blending coefficients. With all coefficients c_k set to zero, we obtain the rest-pose, typically representing a neutral facial expression. In a basic linear blendshape model, all c_k are directly driven by the animator. However, the well-known limitations of linear blending lead to dissatisfying results for some combinations of c_k values. To avoid this problem, artists typically do not modify the c_k coefficients directly, but create a function known as a “rig” that takes as input a reduced, animator-friendly set of control values and outputs all of the c_k coefficients. These controls are typically FACS-based [Ekman and Friesen 1978] and low-dimensional (about 40 to 80 controls), while the c_k coefficients are more numerous (200 to 300, or more in film-quality models). The rig function is typically made from elementary non-linear blocks supporting intermediate and combination (or “corrective”) shapes. The details are not important in this paper but are well explained in the literature [Lewis et al. 2014].

2.2 Linear Blend Skinning

Linear blend skinning has been originally developed for smooth deformations of articulated meshes [Magnenat-Thalmann et al. 1988], but it is a general deformation model [Jacobson et al. 2011]:

$$\sum_{j=1}^P w_{i,j} \mathbf{M}_j \mathbf{v}_{0,i} \quad (2)$$

where $\mathbf{v}_{0,i} \in \mathbb{R}^4$ is $\hat{\mathbf{v}}_{0,i}$ but with the additional coordinate set to 1; $\mathbf{M}_j \in \mathbb{R}^{3 \times 4}$ are affine transformation matrices, corresponding to either skeletal bones in full-body animation or virtual proxy-bones [James and Twigg 2005]; $w_{i,j}$ are skinning weights satisfying the following constraints; *non-negativity*: $w_{i,j} \geq 0$, *partition of unity*: $\sum_j w_{i,j} = 1$ and *spatial sparsity*: the number of nonzero $w_{i,j}$ for each i is bounded by a constant K . Eq. 2 transforms only vertex positions; normals are often approximated but an accurate and efficient method exists [Tarini et al. 2014].

The transformations \mathbf{M}_j are the only time-varying parameters in an animation and thus play the same role as the c_k coefficients in blendshape models (Eq. 1). To convert a blendshape model to a skinned one, we will need a way to convert c_k into \mathbf{M}_j . To our knowledge, this conversion method has not been presented in the literature; skinning decomposition papers [James and Twigg 2005; Le and Deng 2012] assume general animated meshes and provide only playback functionality – they do not discuss the specifics of facial models and the combination of blendshapes represented by skinning transformations.

3 FRAMEWORK

We start by writing down the formula for converting c_k into \mathbf{M}_j . This will also help clarify the framework of our approach and explain the setup for our new *compressed skinning decomposition* algorithm (Sec. 4).

We introduced the problem of *skinning decomposition* via a succinct abstraction using matrices $\mathbf{A} \in \mathbb{R}^{3S \times N}$, $\mathbf{B} \in \mathbb{R}^{3S \times 4P}$ and $\mathbf{C} \in \mathbb{R}^{4P \times N}$. The matrix \mathbf{A} contains $\hat{\mathbf{v}}_{k,i} - \hat{\mathbf{v}}_{0,i}$ and the matrices \mathbf{B}, \mathbf{C} have the following structure:

$$\mathbf{B} = \begin{bmatrix} \hat{\mathbf{N}}_{1,1} & \dots & \hat{\mathbf{N}}_{1,P} \\ \dots & \dots & \dots \\ \hat{\mathbf{N}}_{S,1} & \dots & \hat{\mathbf{N}}_{S,P} \end{bmatrix}, \mathbf{C} = \begin{bmatrix} w_{1,1}\mathbf{v}_{0,1} & \dots & w_{N,1}\mathbf{v}_{0,N} \\ \dots & \dots & \dots \\ w_{1,P}\mathbf{v}_{0,1} & \dots & w_{N,P}\mathbf{v}_{0,N} \end{bmatrix} \quad (3)$$

The matrices $\hat{\mathbf{N}}_{k,j} \in \mathbb{R}^{3 \times 4}$ are defined as $\hat{\mathbf{N}}_{k,j} = \mathbf{I} + \mathbf{N}_{k,j}$, where $\mathbf{I} \in \mathbb{R}^{3 \times 4}$ is a 3×3 identity matrix extended with a column of zeros. With this notation, the formula $\mathbf{BC} = \mathbf{A}$ is equivalent to:

$$\sum_{j=1}^P w_{i,j} (\mathbf{I} + \mathbf{N}_{k,j}) \mathbf{v}_{0,i} = \hat{\mathbf{v}}_{k,i} \quad (4)$$

Due to the fact that $\sum_j w_{i,j} \mathbf{I} \mathbf{v}_{0,i} = \hat{\mathbf{v}}_{0,i}$ which follows from the partition of unity of the skinning weights, Eq. 4 is also equivalent to:

$$\sum_{j=1}^P w_{i,j} \mathbf{N}_{k,j} \mathbf{v}_{0,i} = \hat{\mathbf{v}}_{k,i} - \hat{\mathbf{v}}_{0,i} \quad (5)$$

which shows that the transformations $\mathbf{N}_{k,1}, \dots, \mathbf{N}_{k,P}$ represent exactly the k -th delta-shape $\hat{\mathbf{v}}_{k,i} - \hat{\mathbf{v}}_{0,i}$ (Eq. 1). Intuitively, the subtraction of the identities \mathbf{I} corresponds to subtraction of the rest pose. This is related to the fact that linear blend skinning returns the rest-pose for *identity* transformations, while Eq. 1 returns the rest-pose for *zero* blendweights c_k .

Let us now assume that we have solved for $w_{i,j}$ and $\mathbf{N}_{k,j}$ that satisfy Eq. 5 and all of the skinning weight constraints (this will be discussed in more detail in Sec. 4). Now we just need a formula to compute the final skinning transformations. This formula can be derived by algebraic manipulations of Eq. 1:

$$\begin{aligned} \hat{\mathbf{v}}_{0,i} + \sum_{k=1}^S c_k (\hat{\mathbf{v}}_{k,i} - \hat{\mathbf{v}}_{0,i}) &= \hat{\mathbf{v}}_{0,i} + \sum_{k=1}^S c_k \sum_{j=1}^P w_{i,j} \mathbf{N}_{k,j} \mathbf{v}_{0,i} \\ &= \sum_{j=1}^P w_{i,j} \left(\mathbf{I} + \sum_{k=1}^S c_k \mathbf{N}_{k,j} \right) \mathbf{v}_{0,i} \end{aligned} \quad (6)$$

Therefore, if we define the final skinning transformations \mathbf{M}_j as:

$$\mathbf{M}_j = \mathbf{I} + \sum_{k=1}^S c_k \mathbf{N}_{k,j} \quad (7)$$

for $j = 1, \dots, P$, the linear blend skinning formula (Eq. 2) produces the exact same result as the blending of the blendshapes, as shown in Eq. 6.

The flowchart of our method is in Figure 2. A limitation of our method compared to a standard skinning implementation is the need to evaluate Eq. 7 on the CPU. In the case of dense $\mathbf{N}_{k,j}$, as with Dem Bones implementation, this is a dense matrix-vector product. We propose sparse $\mathbf{N}_{k,j}$ in which case this becomes a sparse matrix-vector product. In either case, the resulting \mathbf{M}_j are dense and are passed to a standard skinning shader. In typical character animation systems, facial animation is usually composited with a head (or neck) transformations and full-body skinning. This can be accomplished by multiplying our \mathbf{M}_j with the head transformation on the CPU, as in standard hierarchical skeletal animation.

In summary, we have converted the delta-blendshape model (Eq. 1) to linear blend skinning. This conversion is exact only if Eq. 5 is satisfied exactly; in practice there will be some errors, but we will minimize them to ensure a visually pleasing approximation of the original blendshape model. Our key contribution (and the rationale behind the name ‘‘Compressed Skinning’’) is that most of our final $\mathbf{N}_{k,j}$ transformations will be zero, enabling us to realize significant savings compared to dense methods such as Dem Bones.

3.1 Transformation representation

The most general choice for $\mathbf{N}_{k,j}$ are general $\mathbb{R}^{3 \times 4}$ matrices, but some authors proposed restricting the 3×3 components to rotations [Le and Deng 2012]. This works well for general animation sequences which are *not* driven by delta-blending, but our approach relies on the linear blending in Eq. 7. Even if we constrained $\mathbf{N}_{k,j}$ to rotations, the resulting \mathbf{M}_j will *not* be rotations due to Eq. 7. Therefore, in our final method we chose to use the following class of transformations:

$$\mathbf{N}_{k,j} = \begin{pmatrix} 0 & -r_{k,j,3} & r_{k,j,2} & t_{k,j,1} \\ r_{k,j,3} & 0 & -r_{k,j,1} & t_{k,j,2} \\ -r_{k,j,2} & r_{k,j,1} & 0 & t_{k,j,3} \end{pmatrix} \quad (8)$$

using only three degrees of freedom for the linearized rotation ($r_{k,j,;}$) [Goldstein et al. 2002] and another three for the translation ($t_{k,j,;}$). This class of transformations is closed under linear blending, i.e., linear combination of transformations of the form of Eq. 8 produces another transformation of the same form. This means that Eq. 7 can work with the 6-dimensional representation in Eq. 8 and compute nothing but plain linear blending at run-time. This is faster than e.g. quaternion interpolation of rotations, which requires a projection/normalization step and safeguards to ensure shortest-path interpolation [Buss and Fillmore 2001]. In our case, linear blending is correct because the original blendshapes were designed to be blended linearly (Eq. 1); non-linearities such as jaw opening are handled in the rig, which we treat as a black box. This is an efficient approach to convert blendshape models into linear blend skinning which also lends itself to a well structured code.

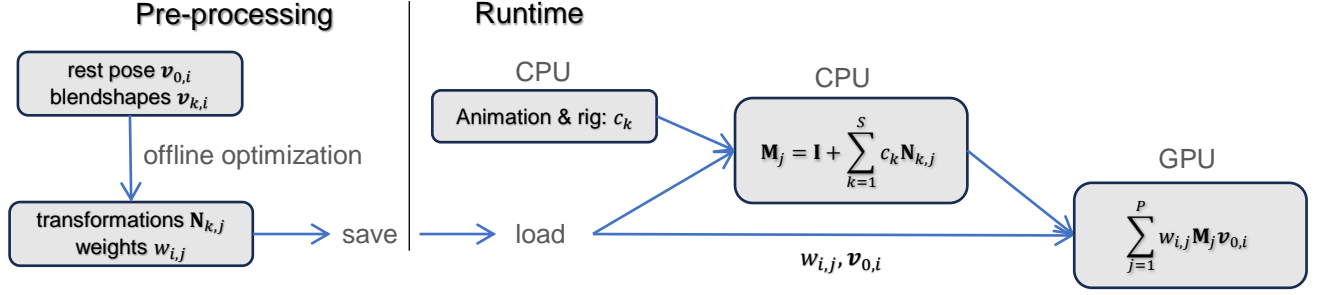


Figure 2: The skinning decomposition is pre-computed offline (left). On the end-user device, we first load the pre-computed $w_{i,j}$ and $N_{k,j}$. Then, for each animation frame (runtime, right), we obtain c_k from the rig and compute M_j . The skinning transformations M_j along with the rest-pose $v_{0,i}$ and weights $w_{i,j}$ are passed to linear blend skinning module running on the GPU.

4 COMPRESSED SKINNING DECOMPOSITION

In this section we discuss the details of our skinning decomposition (Figure 2: pre-processing). This is a non-convex optimization problem:

$$\min_{w_{i,j}, N_{k,j}} \sum_{i=1}^N \sum_{k=1}^S (E_{i,k})^p, E_{i,k} = |v_{k,i} - v_{0,i} - \sum_j w_{i,j} N_{k,j} v_{0,i}| \quad (9)$$

where by default we use $p = 2$ corresponding to the standard Euclidean norm, in which case the absolute value in the definition of $E_{i,k}$ is moot.

Eq. 9 is straightforward to implement in PyTorch, please see the attached code (function compBX). However, an important feature of the skinning decomposition are the following constraints imposed on $w_{i,j}$: non-negativity, partition of unity and spatial sparsity (Sec. 2.2). The spatial sparsity ensures the sparsity of C , which is a classical feature of skinning decomposition [James and Twigg 2005]. On the other hand, the sparsification of B is a new contribution in this paper and we will discuss it in more detail below. To ensure that the skinning approximation is smooth, we also add a Laplacian regularization term, the same as used in previous work [Le and Deng 2014] and in the open source Dem Bones implementation.

Our plan is to leverage the well established Adam optimizer, but the problem is that it is an unconstrained optimizer. In order to incorporate the skinning weight constraints, we draw inspiration from proximal algorithms [Parikh et al. 2014]. The partition of unity constraints are easy: for each vertex i , we simply normalize the weights vector $w_{i,\cdot}$, which ensures that $\sum_j w_{i,j} = 1$. The non-negativity and spatial sparsity constraints can be both satisfied by a single projection (proximal operator for an indicator function): for each weight vector $w_{i,\cdot}$, we keep only the K largest weights and zero out the negative ones. This is conveniently and efficiently implemented by a single call of the `torch.topk` function. This projection is performed after the Adam optimizer step and does not participate in auto-differentiation (in PyTorch this is accomplished via `torch.no_grad`).

With $p = 2$, Eq. 9 is equivalent to the optimization problem solved by Dem Bones [Le and Deng 2012] and our approach converges to solutions with similar errors as the open source Dem Bones

solver. The key advantage of our approach is the ease with which we can add additional constraints or change the loss function. We found that we can achieve significant savings by imposing sparsity constraints also on the B matrix (the sparsity of C is standard in all skinning decomposition methods). We implement this additional sparsity constraint by another projection step, which consists in zeroing-out all but the largest L elements of B in absolute value. The absolute value is necessary because we need to allow negative values in the skinning transformations. Another difference to the C -sparsity case is that with B , we can distribute the non-zeros arbitrarily in the B matrix, whereas the C limits the non-zeros to K per column, due to the limitations of GPUs and standard skinning pipelines. However, the `torch.topk` function applied to $B.abs()$ still works even in the case of the global (as opposed to per-column) budget of non-zero coefficients. In our experiments we typically set L to 6000, which corresponds to 1000 transformations in the representation according to Eq. 8. This is less than 10% of the transformations used by Dem Bones, but we are still able to get similar or even better accuracy (Sec. 5).

4.1 High Detail (HD) Fit

The flexibility of the PyTorch implementation invites experimentation with different values of p in Eq. 9, corresponding to different norms. A particularly interesting case is $p = \infty$, in which case Eq. 9 minimizes the *maximal* deviation from the ground truth blendshapes. We call this the “HD” (High Detail) setting because the infinity norm is more detail-sensitive. Naively using the infinity norm (`max`) actually works, but the convergence is extremely slow because only the vertex with the maximal error generates non-zero gradients. Instead, we can approximate the infinity norm with an L^p norm with a high p ; experimentally, we found that $p = 12$ works well if the model has enough capacity in terms of the number of non-zeros in B, C . However, in our primary goal of reducing the compute overheads by maximizing the sparsity of B, C , we found that higher p can produce non-smooth results; therefore, we use $p = 2$ by default.



Figure 3: Our method leads to results of acceptable visual quality on various rigs and facial expressions, with errors comparable to Dem Bones (red color corresponds to error of 5mm or more). However, our method enables more efficient run-time.

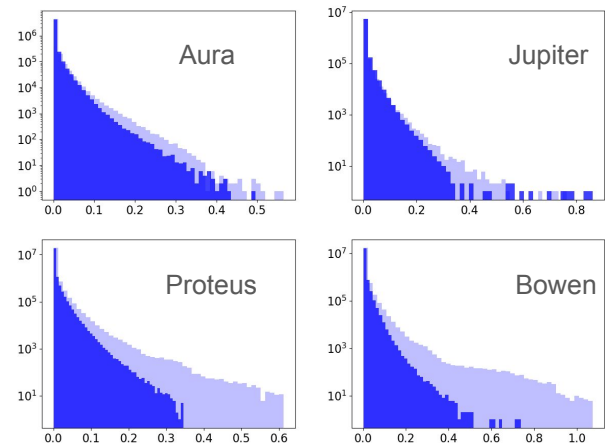


Figure 4: Histograms of the errors of our method (dark blue) and Dem Bones (light blue) in centimeters. Our method achieves lower errors despite sparse skinning transformations.

5 RESULTS

We use two error metrics to quantify the accuracy of a skinning decomposition; mean absolute error (MAE) and maximum absolute error (MXE). The MAE is the mean of $E_{i,k}$ (Eq. 9) and tells us what error can we expect for a randomly chosen vertex and blendshape. The $\text{MXE} = \max_{i,k} E_{i,k}$ measures the worst error. These metrics correspond to L^1 and L^∞ norms. Note that in our task, we assume that our input blendshapes have been carefully prepared and are thus treated as noise-free ground truth, i.e., we cannot dismiss large errors as outliers.

In our first set of experiments, we set the total number of proxy-bones to 40 for both Dem Bones and our method, but we limit our method to no more than 6000 non-zeros in the matrix \mathbf{B} . This means that our method has about $10\times$ fewer transformations to work with than Dem Bones, while achieving similar or better MAE and MXE (Table 1). We set the number of influences K to 8 for both Dem Bones and our method. Rendering of the resulting shapes confirms that the results of Dem Bones and our method are visually similar (Figure 3) and even harder to discern in an animation (see the accompanying video). We plot the corresponding error histograms in Figure 4.

To optimize our compressed skinning decompositions, we used 20k iterations of Adam with projection (Sec. 4) with $\text{lr} = 10^{-3}$, $\beta_1 = 0.9$, $\beta_2 = 0.9$; the whole optimization takes several minutes on a single A6000 GPU. Dem Bones runs in under a minute on the CPU. The pre-processing times are relatively unimportant compared to the reduction of the run-time overhead of blending skinning transformations (Eq. 7). This formula can be expressed as matrix multiplication of the coefficients c_k with the matrix \mathbf{B} . With our method, the \mathbf{B} is sparse, but with Dem Bones and other previous methods, the matrix \mathbf{B} is dense. Sparse matrix data structures (we use compressed row storage) need to store additional index information; we account for these in Table 2. Despite this, sparse data structures offer 5 - $7\times$ memory savings. In Table 3, we report the run-time performance measured on Snapdragon 652, which is

Table 1: Statistics of our testing rigs and achieved fitting accuracy for our method and Dem Bones. Both the maximum (MXE) and mean (MAE) errors are in millimeters, with human-sized head models.

Model	Vertices (N)	Shapes (S)	Bones (P)	Our method			Dem Bones		
				Transforms	MXE	MAE	Transforms	MXE	MAE
Aura	5944	267	40	1000	5.82	0.0384	10680	5.65	0.0391
Jupiter	5944	319	40	1000	8.26	0.0297	12760	7.64	0.0263
Proteus	23735	287	40	1000	4.8	0.03	11480	6.23	0.0305
Bowen	23735	253	40	1000	5.99	0.0339	10120	10.75	0.0459
Proteus HD	23735	287	200	57400	0.06	0.0147	57400	3.45	0.0174

a representative of our target low-spec mobile platforms. We can see that in addition to the memory savings, sparse storage offers also about 2 - 3 \times speed-up and brings the transformation blending times on par with rig evaluation (Table 3). To put the timings in context, with 120Hz refresh rate, the total time budget for a frame is only about 8ms and this needs to accommodate everything, including full-body animation, rendering, background and typically also multiple characters.

Table 2: Memory requirements for sparse (our method) and dense transformations (Dem Bones), using 40 bones in both cases.

Model	Sparse	Dense	Ratio
Aura	81k	512k	6.3 \times
Jupiter	85k	612k	7.2 \times
Proteus	85k	551k	6.5 \times
Bowen	87k	486k	5.6 \times

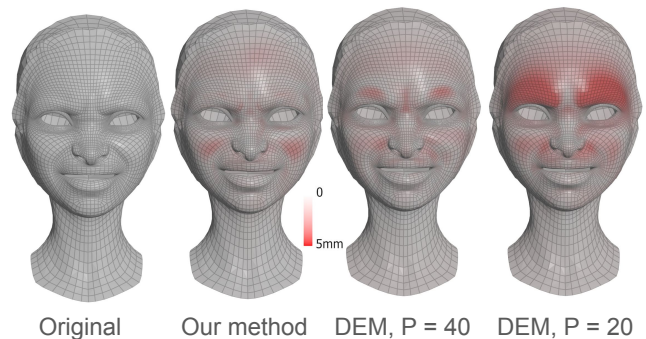
Table 3: Run-time speed measurements for sparse (our method) and dense transformations (Dem Bones), using 40 bones in both cases. We also report the rig evaluation time.

Model	Rig	Sparse	Dense	Speed-up
Aura	164 μ s	160 μ s	552 μ s	3.5 \times
Jupiter	274 μ s	251 μ s	653 μ s	2.6 \times
Proteus	201 μ s	171 μ s	585 μ s	3.4 \times
Bowen	159 μ s	185 μ s	520 μ s	2.8 \times

Another option to consider instead of our method would be to decrease the number of bones P in Dem Bones. We tried this with $P = 20, 10, 5$ and even 1 (i.e., single transformation for the entire model, which we tried just out of curiosity, the visual quality is of course insufficient). The results are in Table 4. We can see the errors increase rather quickly, e.g., with the Aura model, the MXE increased from 0.565 ($P = 40$) to 0.89 ($P = 20$) and the MAE increases similarly from 0.00391 to 0.0058 (Figure 5). Our method enables run-time efficiencies while achieving similar or even lower errors than Dem Bones.

Another potential alternative to our method is to sparsify the skinning transformations after they have been computed by Dem

Bones [Electronic Arts [n. d.]]. To evaluate this approach, we have selected thresholds to zero-out translations and rotations to obtain similar sparsity as our method; specifically we have set the translation threshold as 1mm and the rotation threshold as 1 degree. These sparsified transformations lead to MAEs which are 1.5 to 3 times larger than our method (Table 5).

**Figure 5: Decreasing the number of bones in Dem Bones from 40 to 20 increases the error significantly.**

In our “High-Detail” experiment, we tried to minimize MXE by setting $p = 12$ in Eq. 9, using 200 proxy-bones, disabling the sparsification of our transformations and setting K to 32. We used the same settings in Dem Bones and set smoothness to zero to achieve the highest accuracy. We used 500k iterations (2.5 hours on an A6000 GPU); Dem Bones still uses only about a minute on the CPU. The error metrics, reported as “Proteus HD” in Table 1, show that our $p = 12$ minimization achieved more than 50 \times lower maximal error (MXE) than Dem Bones. The MAE errors are very similar (0.00147 vs. 0.00174), suggesting that the maximal error is well localized. The visual impact of the larger MXE error is loss of details, such as the wrinkles caused by frowning (Figure 6).

We have also implemented our method in Unity and benchmarked the runtimes on a modern Windows PC (AMD 3975WX and NVIDIA RTX 3080). To stress-test the system, we are displaying 10 copies of each of our 4 characters (Figure 7). Since both the CPU and GPU run concurrently, the final FPS is determined by the slower one; in all of our scenarios the CPU is the bottleneck (Table 6). Our method is 1.4 times faster than Dem Bones as well

as Unity’s native implementation of blendshapes. This implementation is optimized for cache coherency etc., but requires 4.2 times longer GPU compute.

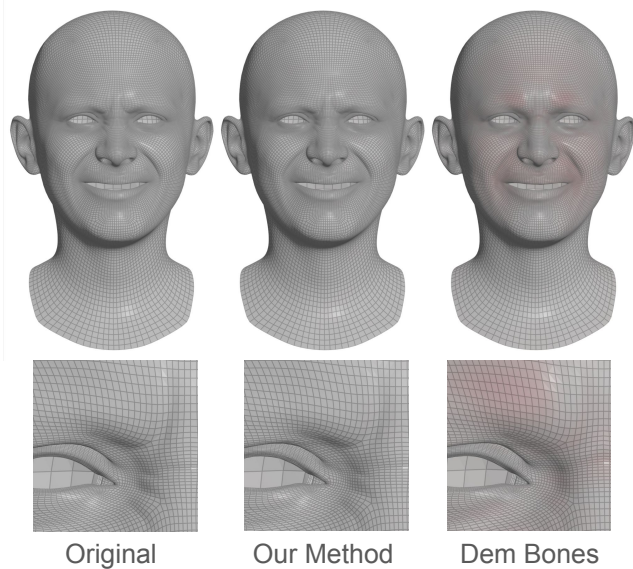


Figure 6: “Proteus HD” experiment: our method with 57400 transforms and L^{12} norm captures finer detail than Dem Bones with the same number of transformations.

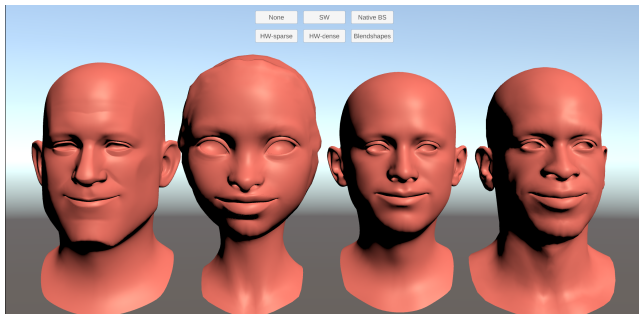


Figure 7: Screenshot of our Unity app.

Table 4: Dem Bones results with lower numbers of bones P (MXE / MAE in millimeters).

Model	$P = 20$	$P = 10$	$P = 5$	$P = 1$
Aura	8.9 / 0.058	21.0 / 0.096	21.2 / 0.113	33.7 / 0.225
Jupiter	10.7 / 0.045	11.6 / 0.063	11.8 / 0.077	31.2 / 0.155
Proteus	11.1 / 0.054	11.4 / 0.070	11.5 / 0.090	29.6 / 0.168
Bowen	9.1 / 0.053	12.9 / 0.089	15.0 / 0.106	33.5 / 0.215

Table 5: Errors with sparsified Dem Bones transformations (40 bones) in millimeters.

Model	Non-zeros	MXE	MAE
Aura	6767	7.46	0.12
Jupiter	5956	10.7	0.040
Proteus	6273	6.12	0.047
Bowen	6520	10.72	0.12

Table 6: Performance on a Windows PC in FPS and milliseconds.

Scenario	FPS	CPU	GPU
Empty scene	2997	0.34	0.05
Our method	252	3.97	1.08
Dem Bones	180	5.35	1.18
Unity blendshapes	185	5.41	4.61

6 CONCLUSION

We have presented a novel method for linear blend skinning decomposition and its integration into a facial animation pipeline. Our new optimization strategy inspired by proximal algorithms outperforms the state-of-the-art and allows us to significantly reduce the run-time overhead of blending skinning transformations, as well as the memory footprint thanks to sparse storage. Alternatively, the benefits of our new optimization method can also be directed towards increasing the fitting accuracy and preserving geometric details. Our meshes contain eye- and mouth-bags and the error is evaluated equally on all vertices. One possible extension of our method would be to introduce importance weighting of individual vertices to e.g. reduce the accuracy on the usually invisible insides of the eyes and the mouth and increase accuracy on more salient parts of the mesh, such as the nasolabial fold.

One limitation of our method are longer pre-processing times due to the first-order optimization approach that requires many iterations. Another limitation is that we consider the rig function as a black box, even though there may be room for further optimizations. In the future, it may be possible to jointly optimize the skinning decomposition along with a neural network approximation of the rig function [Bailey et al. 2020, 2018; Radzihovskiy et al. 2020]; this would require us to adopt new rig evaluation mechanisms, but it could potentially unlock further efficiencies.

ACKNOWLEDGMENTS

We thank Brian Budge, Roman Fedotov, Ryan Goldade, Stephane Grabli, Philipp Herholz, Petr Kadlecek, Binh Le, J.P. Lewis, Ronald Mallet, Olga Sorkine and Yuting Ye for inspiring discussions and the anonymous reviewers for constructive feedback.

REFERENCES

- Michal Aharon, Michael Elad, and Alfred Bruckstein. 2006. K-SVD: An algorithm for designing overcomplete dictionaries for sparse representation. *IEEE Transactions on signal processing* 54, 11 (2006), 4311–4322.
- Stephen W. Bailey, Dalton Omens, Paul Dilorenzo, and James F. O’Brien. 2020. Fast and Deep Facial Deformations. *ACM Transactions on Graphics* 39, 4 (Aug. 2020),

- 94:1–15. <https://doi.org/10.1145/3386569.3392397> Presented at SIGGRAPH 2020, Washington D.C..
- Stephen W Bailey, Dave Otte, Paul Dilonzo, and James F O'Brien. 2018. Fast and deep deformation approximations. *ACM Transactions on Graphics (TOG)* 37, 4 (2018), 1–12.
- Gaurav Bharaj, Thorsten Thormählen, Hans-Peter Seidel, and Christian Theobalt. 2012. Automatically rigging multi-component characters. In *Computer Graphics Forum*, Vol. 31. 755–764.
- Samuel R Buss and Jay P Fillmore. 2001. Spherical averages and applications to spherical splines and interpolation. *ACM Transactions on Graphics (TOG)* 20, 2 (2001), 95–126.
- Prashanth Chandran, Gaspard Zoss, Markus Gross, Paulo Gotardo, and Derek Bradley. 2022. Facial Animation with Disentangled Identity and Motion using Transformers. In *Computer Graphics Forum*, Vol. 41. Wiley Online Library, 267–277.
- Byungkuk Choi, Haekwang Eom, Benjamin Mouscadet, Stephen Cullingford, Kurt Ma, Stefanie Gassel, Suzi Kim, Andrew Moffat, Millicent Maier, Marco Revelant, et al. 2022. Animatomy: An animator-centric, anatomically inspired system for 3d facial modeling, animation and transfer. In *SIGGRAPH Asia 2022 Conference Papers*. 1–9.
- Timothy Costigan, Anton Gerdelan, Emma Carrigan, and Rachel McDonnell. 2016. Improving blendshape performance for crowds with GPU and GPGPU techniques. In *Proceedings of the 9th International Conference on Motion in Games*. 73–78.
- David L Donoho. 2006. Compressed sensing. *IEEE Transactions on information theory* 52, 4 (2006), 1289–1306.
- Paul Ekman and Wallace V Friesen. 1978. Facial action coding system. *Environmental Psychology & Nonverbal Behavior* (1978).
- Electronic Arts. [n. d.]. *Dem Bones: an Open Source Library for Skinning Decomposition*. <https://www.ea.com/seed/news/open-source-dem-bones>
- H. Goldstein, C.P. Poole, and J.L. Safko. 2002. *Classical Mechanics*. Addison Wesley. <https://books.google.ch/books?id=tJCuQgAACAAJ>
- Nils Hasler, Thorsten Thormählen, Bodo Rosenhahn, and Hans-Peter Seidel. 2010. Learning skeletons for shape and pose. In *Proceedings of the 2010 ACM SIGGRAPH symposium on Interactive 3D Graphics and Games*. 23–30.
- Patrik O Hoyer. 2004. Non-negative matrix factorization with sparseness constraints. *Journal of machine learning research* 5, 9 (2004).
- Alec Jacobson, Ilya Baran, Jovan Popovic, and Olga Sorkine. 2011. Bounded biharmonic weights for real-time deformation. *ACM Trans. Graph.* 30, 4 (2011), 78.
- Doug L James and Christopher D Twigg. 2005. Skinning mesh animations. *ACM Transactions on Graphics (TOG)* 24, 3 (2005), 399–407.
- Ladislav Kavan, Rachel McDonnell, Simon Dobbyn, Jiří Žára, and Carol O'Sullivan. 2007. Skinning arbitrary deformations. In *Proceedings of the 2007 symposium on Interactive 3D graphics and games*. 53–60.
- Ladislav Kavan, P-P Sloan, and Carol O'Sullivan. 2010. Fast and efficient skinning of animated meshes. In *Computer Graphics Forum*, Vol. 29. Wiley Online Library, 327–336.
- Joonho Kim and Karan Singh. 2021. Optimizing UI layouts for deformable face-rig manipulation. *ACM Transactions on Graphics (TOG)* 40, 4 (2021), 1–12.
- Diederik P Kingma and Jimmy Ba. 2014. Adam: A method for stochastic optimization. *arXiv preprint arXiv:1412.6980* (2014).
- Binh Huy Le and Zhigang Deng. 2012. Smooth Skinning Decomposition with Rigid Bones. *ACM Trans. Graph.* 31, 6 (2012).
- Binh Huy Le and Zhigang Deng. 2013. Two-layer sparse compression of dense-weight blend skinning. *ACM Transactions on Graphics (TOG)* 32, 4 (2013), 1–10.
- Binh Huy Le and Zhigang Deng. 2014. Robust and accurate skeletal rigging from mesh sequences. *ACM Transactions on Graphics (TOG)* 33, 4 (2014), 1–10.
- Daniel D Lee and H Sebastian Seung. 1999. Learning the parts of objects by non-negative matrix factorization. *Nature* 401, 6755 (1999), 788–791.
- John P Lewis, Ken Anjyo, Taehyun Rhee, Mengjie Zhang, Frederic H Pighin, and Zhigang Deng. 2014. Practice and theory of blendshape facial models. *Eurographics (State of the Art Reports)* 1, 8 (2014), 2.
- Tianye Li, Timo Bolkart, Michael J. Black, Hao Li, and Javier Romero. 2017. Learning a model of facial shape and expression from 4D scans. *ACM Transactions on Graphics, (Proc. SIGGRAPH Asia)* 36, 6 (2017), 194:1–194:17. <https://doi.org/10.1145/3130800.3130813>
- Nadia Magnenat-Thalmann, Richard Laperrire, and Daniel Thalmann. 1988. Joint-dependent local deformations for hand animation and object grasping. In *In Proceedings on Graphics Interface 1988*.
- Peter Melchior, Rémy Joseph, and Fred Moolekamp. 2019. Proximal Adam: robust adaptive update scheme for constrained optimization. *arXiv preprint arXiv:1910.10094* (2019).
- Mark Meyer and John Anderson. 2007. Key point subspace acceleration and soft caching. In *ACM SIGGRAPH 2007 papers*. 74–es.
- Anastasia Moutafidou, Vasileios Toulatzis, and Ioannis Fudos. 2023. Deep fusible skinning of animation sequences. *The Visual Computer* (2023), 1–21.
- Thomas Neumann, Kiran Varanasi, Stephan Wenger, Markus Wacker, Marcus Magnor, and Christian Theobalt. 2013. Sparse localized deformation components. *ACM Transactions on Graphics (TOG)* 32, 6 (2013), 1–10.
- Neal Parikh, Stephen Boyd, et al. 2014. Proximal algorithms. *Foundations and trends® in Optimization* 1, 3 (2014), 127–239.
- Adam Paszke, Sam Gross, Francisco Massa, Adam Lerer, James Bradbury, Gregory Chanan, Trevor Killeen, Zeming Lin, Natalia Gimelshein, Luca Antiga, et al. 2019. Pytorch: An imperative style, high-performance deep learning library. *Advances in neural information processing systems* 32 (2019).
- Sarah Radzihovsky, Fernando de Goes, and Mark Meyer. 2020. Facebaker: Baking character facial rigs with machine learning. In *Special Interest Group on Computer Graphics and Interactive Techniques Conference Talks*. 1–2.
- Scott Schaefer and Can Yuksel. 2007. Example-based skeleton extraction. In *Symposium on Geometry Processing*. 153–162.
- Jaewoo Seo, Geoffrey Irving, John P Lewis, and Junyong Noh. 2011. Compression and direct manipulation of complex blendshape models. *ACM Transactions on Graphics (TOG)* 30, 6 (2011), 1–10.
- Marco Tarini, Daniele Panozzo, and Olga Sorkine-Hornung. 2014. Accurate and efficient lighting for skinned models. In *Computer Graphics Forum*, Vol. 33. Wiley Online Library, 421–428.
- Robert Tibshirani. 1996. Regression shrinkage and selection via the lasso. *Journal of the Royal Statistical Society Series B: Statistical Methodology* 58, 1 (1996), 267–288.